Spliceosomal intronogenesis

Sujin Lee[a] and Scott W. Stevens[b,c,1]

[a]Graduate Program in Cellular and Molecular Biology, The University of Texas at Austin, Austin, TX 78712; [b]Department of Molecular Biosciences, The University of Texas at Austin, Austin, TX 78712; and [c]Institute for Cellular and Molecular Biology, The University of Texas at Austin, Austin, TX 78712

The presence of intervening sequences, termed introns, is a defining characteristic of eukaryotic nuclear genomes. Once transcribed into pre-mRNA, these introns must be removed within the spliceosome before export of the processed mRNA to the cytoplasm, where it is translated into protein. Although intron loss has been demonstrated experimentally, several mysteries remain regarding the origin and propagation of introns. Indeed, documented evidence of gain of an intron has only been suggested by phylogenetic analyses. We report the use of a strategy that detects selected intron gain and loss events. We have experimentally verified, to our knowledge, the first demonstrations of intron transposition in any organism. From our screen, we detected two separate intron gain events characterized by the perfect transposition of a reporter intron into the yeast genes *RPL8B* and *ADH2*, respectively. We show that the newly acquired introns are able to be removed from their respective pre-mRNAs by the spliceosome. Additionally, the novel allele, *RPL8Bint*, is functional when overexpressed within the genome in a strain lacking the Rpl8 paralogue *RPL8A*, demonstrating that the gene targeted for intronogenesis is functional.

spliceosome | intron | evolution

One of the defining features of all eukaryotic organisms is the presence of intervening sequences termed introns in at least some nuclear genes (1, 2). The removal of introns from eukaryotic pre-mRNA within the spliceosome is mechanistically related to self-cleaving group II introns from prokaryotes and eukaryotic organelles (3–5) (Fig. S1). Although much work has been done in examining the mechanism and machinery of spliceosomal intron removal (1, 2), several evolutionary mysteries remain regarding introns: How did spliceosomal introns invade and persist in eukaryotic genomes? How are they removed from the genomes of organisms undergoing intron loss? Have introns been added over evolutionary time, and if so, how does that occur?

Several models exist for how introns might be lost (6–8), and experimental intron loss has been demonstrated in at least one organism (9, 10) (Fig. S2). Indeed, at this time in evolution, budding yeast is a species in which widespread intron loss has been proposed to have occurred, likely through RNA-mediated homologous recombination of cDNA (9, 11). This model is likely to be correct, as it reflects the genomic reality that budding yeast introns generally exist close to the 5′ end of intron-containing genes, as would be expected in a reaction mediated by reverse transcriptase, which begins copying the mRNA from the 3′ end (7, 12–14).

Models for how introns are gained are numerous, however no model has yet been experimentally validated (15, 16). These models include intron transposition, intron gain during double-stranded DNA break repair, transfer of an intron from a paralogous gene, and an appealing model involving reverse-splicing. This model invokes the incorporation of an intron retained in the residual spliceosome into an intron-naïve mRNA that has encountered and stably interacted with this species (17) (Fig. S3). Although all of these models could potentially lead to intronogenesis, none have yet been demonstrated in vivo.

Most of the published work on the phenomena of intron gain and loss has used phylogenetic comparisons of intron presence and position across intron-containing genes, made possible by the existence of extensive genome sequence databases (16). Definitive conclusions of intron gain or loss are difficult to make by these analyses, however

it is clear that introns massively infiltrated the genome of the last eukaryotic common ancestor and that introns have continued to be gained and lost over evolutionary time (11, 18).

Here we report the use of a reporter system designed to detect events of intron gain and intron loss in the budding yeast *Saccharomyces cerevisiae*. With this reporter, we have captured, to our knowledge, the first verified examples of intron gain via intron transposition in any eukaryote.

Results

The design of the reporter is outlined in Fig. 1A. In this construct, which has been modified from one used previously in our other work (19), the intron and short stretches of exons 1 and 2 of the *RPL28* gene (ribosomal protein L28) have been fused in-frame to EGFP (enhanced green fluorescent protein). Within the intron, we have used the heterologous *Schizosaccharomyces pombe TEF1* promoter to drive transcription of the *S. pombe his5+* gene, which confers histidine prototrophy in *S. cerevisiae his3* mutants. The transcriptional direction of *his5+* is in the opposite orientation to that of the EGFP construct. Within the *his5+* gene, we have inserted an artificial intron (modeled on those described in refs. 9 and 20) containing pre-mRNA splicing signals that are only capable of being spliced from the EGFP transcript but not from the *his5+* transcript. Verification of the proper splicing of this reporter by virtue of EGFP protein production is shown in Fig. 1B. The array of recursive splicing products was also tested by RT-PCR and sequence analysis of the PCR products (Fig. S4). We note that similar to our previous work with a related construct (19), this intron is poorly spliced, however there is reasonably good EGFP splicing and EGFP protein production.

This reporter is conceptually related to ones used previously to detect de novo Ty1 retrotransposition events (20) and RNA-mediated intron loss (9); however, the selection signal for the other reporters was contained on the resulting mRNA, whereas this reporter selection signal is contained within the spliced

---

Significance

Eukaryotic transcripts contain spliceosomal introns that need to be removed by pre-mRNA splicing. Although several models have been proposed to identify the mechanism of intron gain over the evolution of eukaryotes, they remain models due to a lack of experimental validation. We developed a reporter system to detect selected intron gain and loss events and captured two intron gain events in which the intron derived from the reporter was transposed into the chromosomal loci of *RPL8B* and *ADH2*. This is, to our knowledge, the first demonstration of intron gain via intron transposition in any organism, and we suggest that these events are likely to have occurred by a reversal of the pre-mRNA splicing reaction followed by homologous recombination.
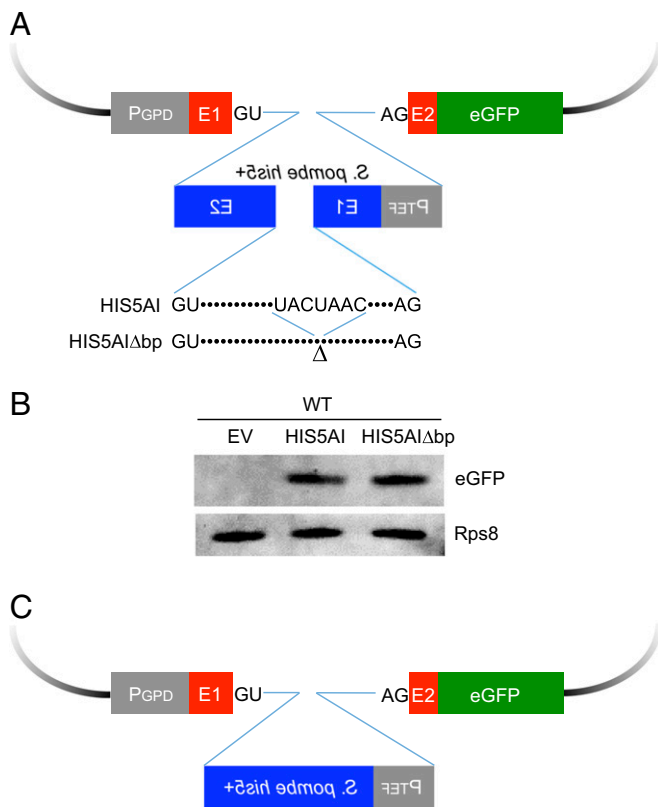

Fig. 1. Design and splicing of the intron gain/loss reporter. (*A*) Model of the intron gain/loss reporter. Short stretches of exon 1 and exon 2 of the *RPL28* gene with portions of the intron were fused to EGFP. The *S. pombe his5*+ gene was inserted into the *RPL28* intron (EGFP gene). Backwards text represents the opposite transcriptional orientation of the *S. pombe his5*+ gene. The *his5*+ gene was interrupted by an artificial intron (AI) containing splice sites that are only spliced from the EGFP transcript, due to their orientation. The AI lacking the branch point sequence (AIΔbp) cannot be spliced from the EGFP transcript. After splicing of the artificial intron followed by RNA-mediated recombination, transcription of *S. pombe his5*+ gene driven by *TEF1* promoter confers histidine prototrophy in *S. cerevisiae his3* mutants. (*B*) Demonstration of EGFP production. Splicing and expression of EGFP from the reporter was demonstrated by Western blot analysis using an antibody to GFP. Western blot analysis of Rps8 was used as a loading control. (*C*) Plasmid-borne intron loss events. The plasmids rescued from most his+ cells have lost the artificial intron within the *S. pombe his5*+ gene.

intron. Intron mobilization leading to histidine prototrophy can be a result of a few key events. The most common event in our screen is plasmid-borne intron loss, related to the RNA-mediated recombination events shown previously (9, 20) (Fig. 1*C*). In this intron loss, the intron within the *his5*+ gene has been spliced out, and a species of the EGFP intron RNA has been reverse-transcribed and recombined back into the reporter plasmid. From these data, it is not possible to determine if this is a singly spliced, intron-containing EGFP pre-mRNA or the liberated EGFP intron that gave rise to these events, however sequencing of the *his5*+ gene in the plasmid revealed that the *his5*+ intron has been precisely removed. As a control, a screen with a reporter construct lacking the branchpoint sequence within the *his5*+ intron produced no histidine prototrophs (Fig. 1*A*), indicating that removal of the artificial intron from the EGFP intron by splicing followed by RNA transposition of the EGFP intron is required for histidine prototroph formation.

Our screen was conducted on nearly 2×10^{11} cells from which we detected ~10,000 plasmid-borne intron loss events, resulting in an RNA-mediated recombination rate similar to that previously reported (9). In addition to the plasmid-related events, we

detected two instances of intron gain that resulted from a perfect chromosomal addition of the EGFP intron into an mRNA-encoding gene. Direct genomic sequencing (21) and inverse PCR from genomic DNA (Fig. S5) in the first captured intron gain strain revealed that an intronogenesis event occurred in the *RPL8B* gene (ribosomal protein L8B) (Fig. 2*A*). PCR amplification and sequencing of the entire *RPL8B* locus confirmed that the transposed intron was inserted 18 nucleotides downstream from the start codon of the gene and that after intron removal from the *RPL8B* pre-mRNA, the resulting mRNA is competent for translation into a proper Rpl8 protein. In the second intron gain strain, the EGFP intron was transposed into the *ADH2* gene (alcohol dehydrogenase), 204 nucleotides downstream from the start codon
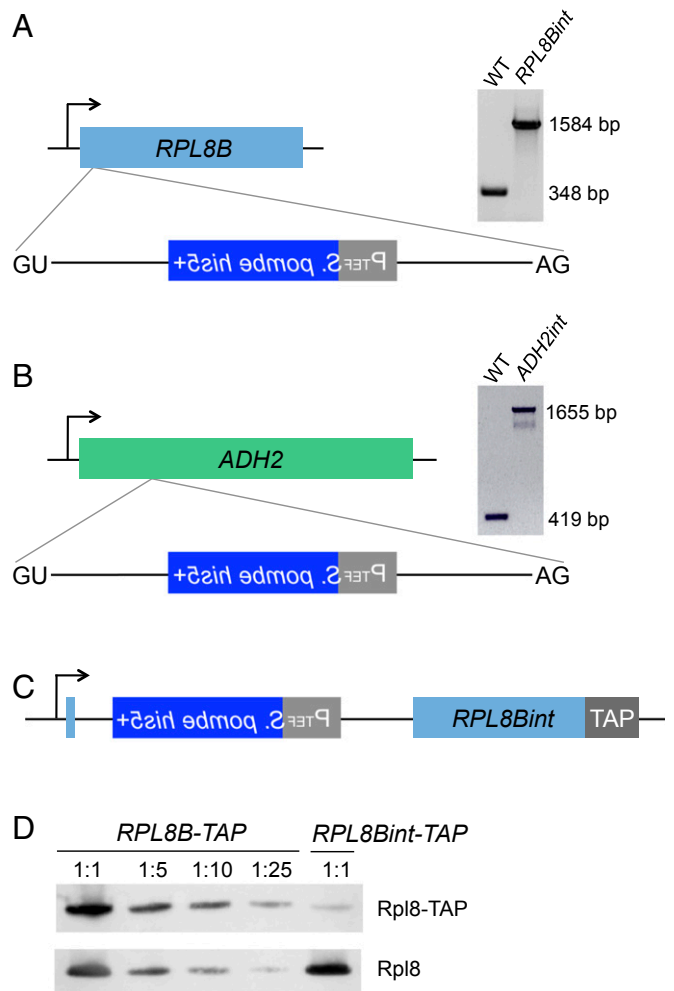

Fig. 2. Transposition of the EGFP intron into the chromosomal locus, leading to a gain of a spliceable intron. (*A*) The *RPL8Bint* locus. (*Left*) The entirety of the EGFP intron (lacking the spliced-out artificial intron) was transposed 18 nucleotides downstream from the start codon of *RPL8B*. It contains all of the pre-mRNA splicing signals required to splice the *RPL8Bint* transcript. (*Right*) PCR products of the *RPL8B* locus from genomic DNA of wild-type and *RPL8Bint* strains. The size difference in the PCR products of *RPL8Bint* indicates the acquisition of the reporter intron (1,236 bp) in *RPL8Bint*. (*B*) The *ADH2int* locus. (*Left*) The EGFP intron was inserted 204 nucleotides downstream from the start codon of *ADH2* in the same manner observed in *RPL8Bint*. (*Right*) PCR products of the genomic *ADH2* locus in wild-type and *ADH2int* strains reflect the reporter intron transposition in *ADH2int*. (*C*) TAP tagging of *RPL8Bint*. The TAP tag (22) was inserted into the C terminus of the *RPL8Bint* gene. (*D*) Quantitation of Rpl8 expressed from *RPL8Bint-TAP*. To quantitatively compare Rpl8-TAP protein levels in the indicated strains, *RPL8B-TAP* was serially diluted as shown in the figure. Rpl8 and Rpl8-TAP were detected by an antibody to Rpl8 and quantitated by chemifluorescence.

GENETICS

(Fig. 2B). PCR amplification of genomic DNA and cDNA in this strain demonstrated that the newly formed intron is able to be spliced from the *ADH2* pre-mRNA (Fig. 2B and Fig. S6). The new alleles of *RPL8B* and *ADH2* were termed *RPL8Bint* and *ADH2int*, respectively. Additionally, we observed two events that were not plasmid-borne but that resulted in histidine prototrophy, likely by virtue of nonhomologous recombination of plasmid sequences containing the *his5+* gene from which the intron was previously lost. These two events were not related to the intronogenesis process, as they also included EGFP exon sequences, indicating that the mechanism did not involve the lariat intron (*Discussion*).

The *RPL8Bint* pre-mRNA is spliced, as shown by Western blotting of a strain in which *RPL8Bint* has been tandem affinity purification (TAP) tagged (22) (Fig. 2C). Quantitative comparisons of the levels of the *RPL8B-TAP* (23) to that of *RPL8Bint-TAP* show that Rpl8 protein produced from the *RPL8Bint-TAP* locus is ~2% of that from the *RPL8B-TAP* locus (Fig. 2D). This is most likely due to the inefficient splicing of the very large intron containing the *his5+* gene (19) (Fig. S4). Budding yeast introns are typically much shorter than in other species, and as the size of the intron increases, splicing efficiency dramatically decreases (24). Indeed, at 1,236 nucleotides, this intron is 235 nucleotides longer than the largest natural intron in *S. cerevisiae* (25). Thus, it is not surprising that knocking out the Rpl8 paralog *RPL8A* in *RPL8Bint* proved to be impossible either by direct removal or by crossing and dissection of tetrads.

Because the levels of Rpl8 produced from *RPL8Bint* were so low and because we wished to show that the new intron added to *RPL8B* could suffice for production of Rpl8, we modified both *RPL8Bint* and *RPL8Bint-TAP* to be driven from a strong heterologous promoter derived from the *TDH3* gene (26) (Fig. 3A). This modification restored the levels of Rpl8 to wild-type levels as determined by Western blotting in the *GPD-RPL8Bint-TAP* strain (Fig. 3B). Removal of *RPL8A* from the *GPD-RPL8Bint* strain was achieved by crossing *GPD-RPL8Bint* with the *rpl8A*Δ strain followed by sporulation (Fig. 3C). Indeed, total levels of Rpl8 are very similar in wild-type, *GPD-RPL8Bint*, and *rpl8a*Δ/*GPD-RPL8Bint* strains (Fig. 3D), indicating that the Rpl8 expressed from the *GPD-RPL8Bint* locus is sufficient in these cells. Not only is the expression level comparable to the wild type, Rpl8 in the *rpl8a*Δ/*GPD-RPL8Bint* strain is also fully functional, as it exhibits no detectable growth defects (Fig. S7).

Discussion

Here we report, to our knowledge, the first experimental demonstration of spliceosomal intron transposition in any eukaryotic organism. We detected the insertion of an EGFP reporter intron into the genomic *RPL8B* and *ADH2* using a reporter construct. In our model of *RPL8Bint* formation, the EGFP intron RNA lacking the *his5+* artificial intron was retained in the residual spliceosome after Prp22-mediated mRNA release (Fig. 4). This complex then encountered an *RPL8B* mRNA and inserted the reporter intron by reverse splicing (15, 17). *RPL8Bint* pre-mRNA was then reverse-transcribed by a cellular reverse transcriptase (likely derived from the Ty1 retroelement) (9, 20), and the resulting *RPL8Bint* cDNA was incorporated into the *RPL8B* genomic locus by homologous recombination. We suggest that the formation of *ADH2int* is likely to have occurred by the same model.

It may not be surprising that in ~2 × 10^11 cells we captured only two intron gain events while observing over 10,000 plasmid-borne intron loss events, considering that our model of intron gain involves an additional reverse splicing step that is expected to be rare in vivo (15). Previous work showed the capability of the spliceosome to achieve the reversal of the two catalytic steps of splicing in vitro (17), however those experiments were performed at nonstandard salt and pH conditions to promote the reverse reactions. We would like to point out that the sequences of our reporter construct and the location of insertion in *RPL8B* and *ADH2* do not have even short regions of homology, which could explain this intron gain as
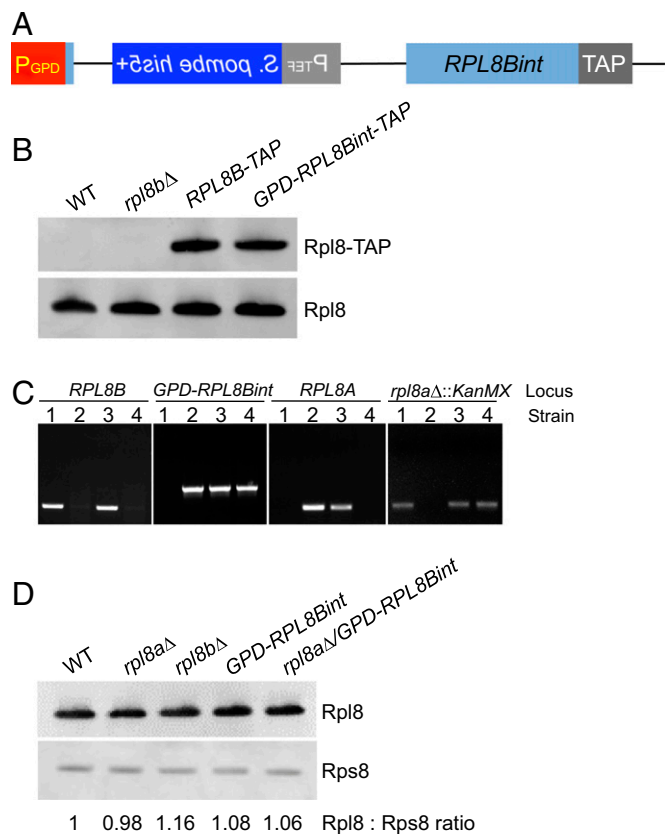

Fig. 3. The *Rpl8Bint* locus is sufficient for Rpl8 production when overexpressed. (*A*) *GPD-RPL8Bint* construction. The original promoter of the *RPL8Bint* and *RPL8Bint-TAP* was replaced with the GPD promoter to increase the expression level. (*B*) Quantitation of Rpl8 expressed from *RPL8B-TAP* to *GPD-RPL8Bint-TAP*. To determine the effect of the GPD promoter, the amount of Rpl8 expressed from *RPL8B-TAP* and *GPD-RPL8Bint-TAP* strains was determined by Western blotting. Rpl8 and Rpl8-TAP were detected by an antibody to Rpl8. (*C*) PCR confirmation of *rpl8a*Δ/*GPD-RPL8Bint* and related strains. Shown is the genomic DNA amplification of a portion of *RPL8B*, *GPD-RPL8Bint*, *RPL8A*, and *rpl8a*Δ::*KanMX* loci from each strain, labeled 1–4 (1, *rpl8a*Δ; 2, *GPD-RPL8Bint*; 3, diploid formed from *rpl8a*Δ and *GPD-RPL8Bint*; 4, haploid *rpl8a*Δ/*GPD-RPL8Bint*). (*D*) Quantitative Western blot. Total levels of Rpl8 were determined in wild-type, *rpl8a*Δ, *rpl8b*Δ, *GPD-RPL8Bint*, and *rpl8a*Δ/*GPD-RPL8Bint* strains by Western blotting using chemifluorescence.

having taken place via a microhomology-based recombination event (27) (Fig. 5A). Interestingly, the four nucleotides in the *RPL8B* transcript at the site of intron insertion (the −3, −2, −1, and +1 positions relative to the intron) possess base-pairing potential with the invariant U5 loop at the proper positions (28, 29) (Fig. 5). Comparable base-pairing potential exists between the four nucleotides in the *ADH2* transcript at the intron junction (−3, −2, −1, and +1) and the U5 loop (Fig. 5). This provides further evidence that reverse splicing may have occurred and suggests that in this mode of intron gain, new mRNAs may be selected for intron addition by the spliceosome at sites at which splicing may be more efficient in the forward reaction (Fig. 4).

Although how the spliceosomal introns emerged and why only eukaryotes possess this class of introns remain unclear, it is widely accepted that the spliceosomal introns originated from the group II self-splicing introns and appeared at the time of eukaryogenesis (11, 18). It is likely that the proto-spliceosomal introns resembled the group II introns and for some period retained their mobility and self-splicing ability (5). This may have enabled and promoted considerable proliferation of these introns at the time of eukaryogenesis (11, 18). The group II intron-derived features are likely to have degenerated over time, leading to a necessity for the development
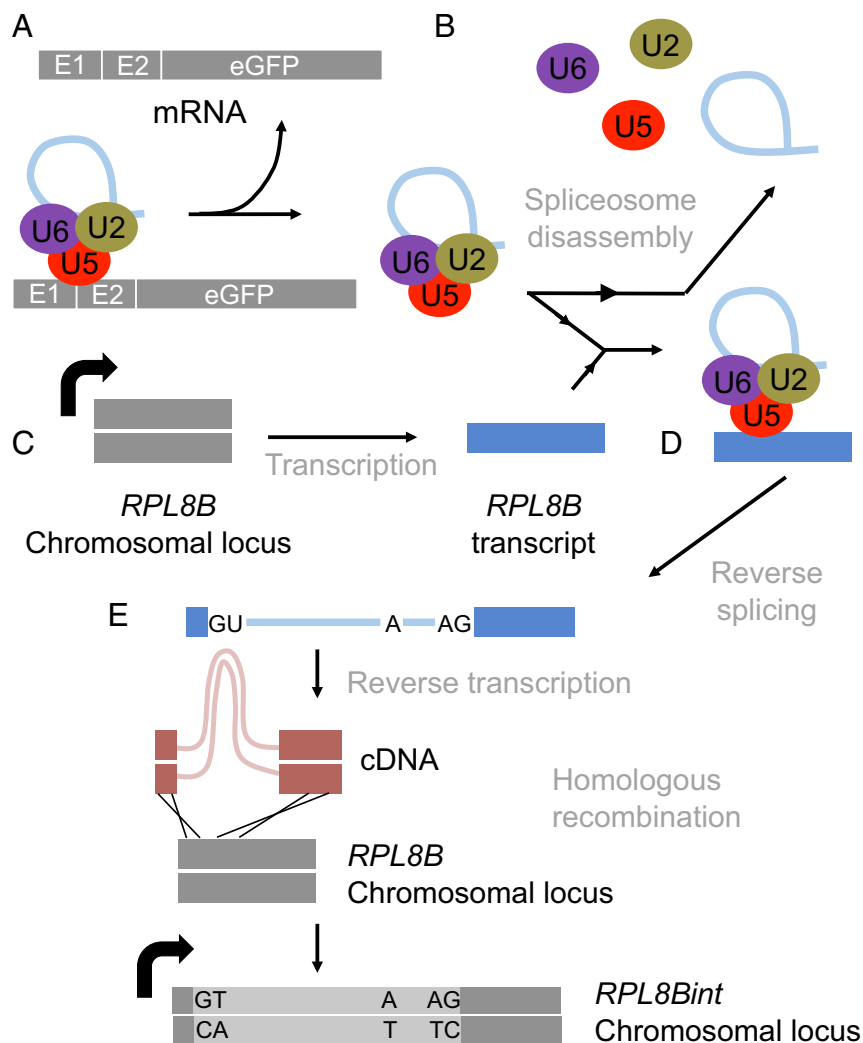
Fig. 4. Proposed model for the mechanism of *RPL8B* intron gain. (*A*) The last step of the pre-mRNA splicing reaction. The spliced mRNA (*Top*) is disengaged from the residual spliceosome composed of the lariat intron; the U2, U5, and U6 snRNPs; and other splicing proteins. (*B*) Disassembly of the residual spliceosome under normal conditions. The U2, U5, and U6 snRNPs and the lariat intron are dissociated from each other at the end of the splicing reaction. (*C*) Transcription of the *RPL8B* mRNA, the proposed substrate for the intron transposition. (*D*) Model of the transposition of the reporter intron contained within the intact residual spliceosome into the *RPL8B* transcript. The *RPL8B* transcript was captured by an intact, lariat intron-containing spliceosome before proceeding through both catalytic steps of pre-mRNA splicing, in reverse (17). (*E*) Proposed mechanism of transposed intron mobilization into the *RPL8B* locus. The transposed reporter intron within the *RPL8B* mRNA underwent a conversion to double-stranded cDNA by a reverse transcriptase, followed by homologous recombination into the genome at the *RPL8B* locus.

of the pre-mRNA splicing machinery composed of trans-acting snRNAs and trans-acting protein factors (11, 18). Within this context, reverse splicing-catalyzed intron transposition is an appealing model for intron gain.

Demonstration of intron gain events in vivo has been a major obstacle to test existing models of intron gain. The in vivo intron gain presented in this work strengthens the intron gain model involving reverse splicing by providing, to our knowledge, the first evidence that it can occur on a laboratory time scale. At this point in the arc of evolution, for an intron gain event to become fixed in a population, either the intron insertion needs to result in a selective advantage to that organism or individuals possessing a new intron insertion event need to find themselves in ecological niches in which they can further speciate. Indeed in recent reports, some intron gain events have been suggested to have occurred by means other than reverse splicing and are highly mosaic depending on the individuals that have been analyzed (30–33), indicating that it may be that there are multiple mechanisms of intron gain that may change over time and genetic circumstance.

Materials and Methods

Experimental Design of a Reporter System. The intron reporter was generated by modification of the splicing reporter used in our previous work (19). The two-color fluorescence reporter containing the *RPL28* intron fused to EGFP and mCherry in the intron (pRS316 backbone) was restriction enzyme-digested with SphI and AflIII to remove the mCherry ORF. A synthetic construct (Genscript) containing the *S. pombe tef1⁺* promoter driving the *S. pombe his5⁺* gene and terminating with the *S. pombe tef1⁺* termination sequence was cloned into those same restriction sites.

Yeast Strains. SS4056 (parent BY4739) (MATα *his3::KanMX, leu2Δ0, lys2Δ0, ura3Δ0*), BY4733 (MATa *his3Δ200, leu2Δ0, met15Δ0, trp1Δ63, ura3Δ0*), and SS4019 (parent BY4741) (MATa *his3Δ1, leu2Δ0, met15Δ0, ura3Δ0, trp1Δ*) were used for intron transposition assays. SS5230 (parent SS4056) (MATα *his3::KanMX, leu2Δ0, lys2Δ0, ura3Δ0, RPL8B::his5⁺::int*) and SS5252 (MATα *his3::KanMX, leu2Δ0, lys2Δ0, ura3Δ0, ADH2::his5⁺::int*) were obtained by intron gain. SS5231 (MATα *his3::KanMX, leu2Δ0, lys2Δ0, ura3Δ0, RPL8B::his5⁺::int::TAP::HYG*), SS5232 (MATα *his3::KanMX, leu2Δ0, lys2Δ0, ura3Δ0, URA3::GPD-RPL8B::his5⁺::int*), SS5233 (MATα *his3::KanMX, leu2Δ0, lys2Δ0, ura3Δ0, URA3::GPD-RPL8B::his5⁺::int::TAP::HYG*), and SS5235 (MATα *his3::KanMX, leu2Δ0, lys2Δ0, ura3Δ0, rpl8aΔ, URA3::GPD-RPL8B::his5⁺::int*) were generated to further
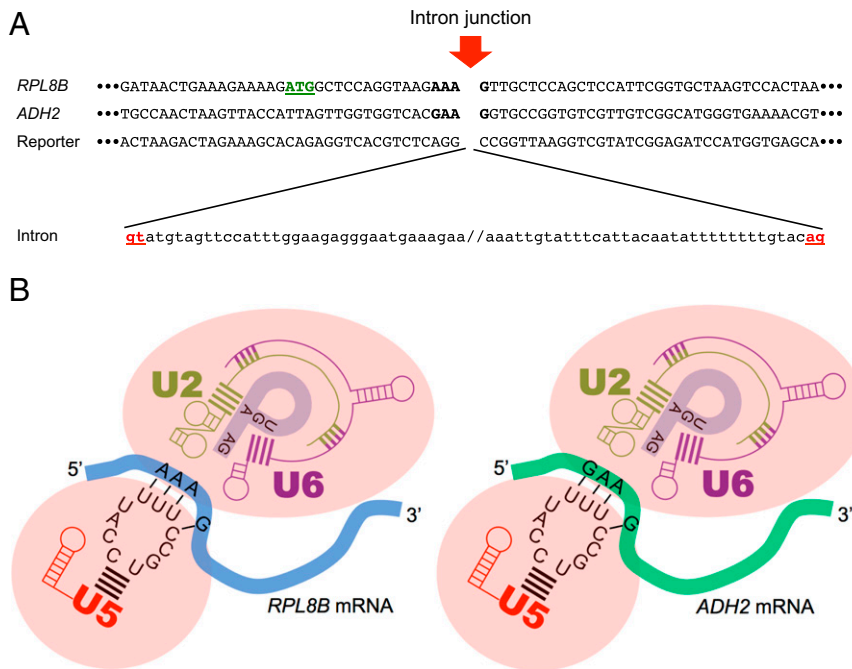
GENETICS

Fig. 5. The sequence information at the intron insertion sites supports an intron gain model involving reverse splicing. (*A*) Microhomology-mediated end-joning rules preclude recombination as a means of this intron acquisition. The coding strand sequences of *RPL8B*, *ADH2*, and the reporter construct at both ends of the inserted intron were juxtaposed to examine the possibility of very short sequence homology. Neither *RPL8B* nor *ADH2* show potential microhomology to the reporter construct at the intron junctions. Note the start codon of *RPL8B* highlighted in green. (*B*) Closer view of the *RPL8B* (*Left*) and *ADH2* (*Right*) transcript engaging with the spliceosome showing the proposed base-pairing interactions between the new splice site and loop 1 of the U5 snRNA. The nucleotides of *RPL8B* and *ADH2* participating in the potential base-pairing are marked in bold in *A*.

analyze the *RPL8Bint* strain. *RPL8B-TAP*–tagged strain (background BY4741) (MATa *his3Δ1*, *leu2Δ0*, *met15Δ0*, *ura3Δ0*, *RPL8B-TAP::HIS3MX6*) (Yeast-TAP–tagged ORF library, GE Dharmacon), *rpl8aΔ* strain (background BY4741) (MATa *his3Δ1*, *leu2Δ0*, *met15Δ0*, *ura3Δ0*, *rpl8a::KanMX*) (GE Dharmacon), and *rpl8bΔ* strain (background BY4741) (MATa *his3Δ1*, *leu2Δ0*, *met15Δ0*, *ura3Δ0*, *rpl8b::KanMX*) (GE Dharmacon) were used to quantitatively analyze Rpl8 expressed in the *RPL8Bint* strains.

Intron Transposition Assay. Yeast cells transformed with pRS416 (empty vector), pRS316HIS5AI, or pRS316HIS5AIΔbp were plated on SD-ura and grown for 72 h at 31 °C. Individual uracil prototrophs were then grown in 10 mL SD-ura liquid medium overnight at 31 °C and cells harvested by centrifugation. Pelleted cells were resuspended in water and plated on 150-mm SD-his plates and grown at 31 °C for 4–6 d. All his+ colonies were patched onto YPD plates, grown overnight at 31 °C, and then streaked on SD-his 5-FOA. After incubation at 31 °C for 6 d, his+ cells were scored for their resistance to 5-FOA.

Inverse PCR. Genomic DNA was isolated from his+/5-FOAr cells and cut sequentially with BstYI and BclI restriction endonucleases. This DNA was phenol-extracted, ethanol-precipitated, and then resuspended in water to be ligated using T4 DNA ligase (New England Biolabs) under conditions favoring self-ligation (9). After overnight ligation at 16 °C, the DNA was extracted, precipitated, and resuspended in 50 μL of water for use in an inverse PCR. DNA was amplified by PCR with primers hybridizing within the reporter intron region using Taq DNA polymerase with ThermoPol buffer (New England Biolabs): SpHIS5iPCR2F, 5′-CCAAGCACGAAGGGAGTGTTGTAAAGTAAC-3′; SpHIS5iPCR3R, 5′-ACATGCAAAGTAATTCCAGC-3′; SpHIS5iPCR3F, 5′-CAAGTAATCCAAGTAGA-CAC-3′; and SpHIS5iPCR2R, 5′- GTTTATGTTCGGATGTGATGTGAG-3′

RPL8Bint and ADH2int Identification and Confirmation by PCR. The intron insertion was first identified by direct genomic DNA sequencing (21) and inverse PCR and confirmed by PCR with the following primer sets, respectively: *RPL8Bint*, 2014.7, 5′-GTATTGTGATGCGCACGTTGAAATTCAC-3′; *RPL8Bint*, 2014.5, 5′-CAG-CGGTGTTTCTGTCCAAAGTG-3′; *ADH2int*, ADH2int RT5, 5′-CAACGGCAAGTTGG-AGCATAAG-3′; ADH2int RT3, 5′-CACACAAGATTGGCGCGACTTCAG-3′.

TAP Tagging of RPL8Bint. The TAP tag was introduced at the C terminus of the genomic *RPL8Bint* locus by homologous recombination with the hygromycin

B-resistant selectable marker adjacent to the TAP cassette (22). Oligonucleotide primers contain a 40-bp-long region identical to the yeast genome for homologous recombination. Primers A and B hybridize at the 5′ end of the CBP (calmodulin binding peptide) coding sequence and at the downstream of the coding sequence of hygromycin B phosphotransferase, respectively: RPL8BtapA-HYG, 5′-AGCTAAGATGGACAAGAGAGCTAAGACTTCCGACTCCGCTATGGAAAAGAGAA-GATGGAA-3′; RPL8BtapBpRS41H, 5′-TACAAAATATAATTATATTACGATGTTCGA-AATTCTATATACTGAGAGTGCAGCGACATG-3′.

RPL8Bint Promoter Switch. The GPD (*TDH3*) promoter was introduced to replace the promoter of *RPL8Bint* at the genomic locus by homologous recombination. Primers contain a 55 nucleotide-long region identical to regions upstream and downstream of the *RPL8Bint* start codon for homologous recombination. Oligonucleotides KIA and KIB were designed to amplify a DNA fragment containing the GPD promoter with the *URA3* marker for selection purposes: RPL8B-GPD-URA-KIA, 5′-ATAGAACGCATTGAAACTTTTCCCATCTCAAAATCCAG-GGACAATAGTATGGGATGCGCGTTTCGGTGATGACGGTG-3′; RPL8Bint-GPD-URA-KIB, 5′-GGTTCTTTCATTCCCTCTTCCAAATGGAACTACATACTTTCTTACCTGGAGCCATT-TTGTTTGTTTATGTGTGTTTATTCG-3′.

Yeast Sporulation and Tetrad Dissection. *GPD-RPL8Bint* (SS5232) and *rpl8aΔ* strains were mixed on an YPD plate within a drop of water, incubated overnight at 31 °C, and then diploids were selected by streaking on SD-his-lys media. The diploid cells were inoculated into 2 mL of SD-his, incubated for 30 h at 31 °C, harvested, and washed with water. The cells were resuspended in 2 mL of SPM (100 mM Potassium acetate and 400 μM Raffinose) and incubated on a roller drum at room temperature for 5 d to sporulate. We treated 100 μL of the sporulated culture with 15 μg of Zymolyase T100 in 20 mM β-mercaptoethanol at 30 °C for 20 min and dissected it on a tetrad dissection microscope.

Protein Isolation and Quantitation. Yeast cells were grown in YPD at 31 °C, and 1 OD unit of the cells was harvested by centrifugation, resuspended in 1 mL of YPD, chilled on ice for 10 min, and then mixed with 150 μL of ice-cold 2 N NaOH and 8% (vol/vol) β-mercaptoethanol. After an additional 10-min incubation on ice, the cells were mixed with 150 μL of ice-cold 50% (vol/vol) TCA, chilled on ice for another 10 min, and harvested by centrifuging at 4 °C at (16,000 × *g*) for 2 min. The pellets were washed with 1 mL of ice-cold acetone

and resuspended in 100 μL of 1× LDS sample buffer containing 100 mM DTT. Extracted protein was subjected to Western blot analysis using a chemi-fluorescence detection kit. Quantitation of proteins in Western blots was performed using the Quantity One analysis software (Bio-Rad) and ImageJ [National Institutes of Health (https://imagej.nih.gov/ij)].

1. Matera AG, Wang Z (2014) A day in the life of the spliceosome. *Nat Rev Mol Cell Biol* 15(2):108–121.
2. Will CL, Lührmann R (2011) Spliceosome structure and function. *Cold Spring Harb Perspect Biol* 3(7):a003707.
3. Cech TR (1986) The generality of self-splicing RNA: Relationship to nuclear mRNA splicing. *Cell* 44(2):207–210.
4. Jacquier A (1990) Self-splicing group II and nuclear pre-mRNA introns: How similar are they? *Trends Biochem Sci* 15(9):351–354.
5. Lambowitz AM, Zimmerly S (2011) Group II introns: Mobile ribozymes that invade DNA. *Cold Spring Harb Perspect Biol* 3(8):a003616.
6. Fink GR (1987) Pseudogenes in yeast? *Cell* 49(1):5–6.
7. Mourier T, Jeffares DC (2003) Eukaryotic intron loss. *Science* 300(5624):1393.
8. Boeke JD, Garfinkel DJ, Styles CA, Fink GR (1985) Ty elements transpose through an RNA intermediate. *Cell* 40(3):491–500.
9. Derr LK, Strathern JN, Garfinkel DJ (1991) RNA-mediated recombination in *S. cerevisiae*. *Cell* 67(2):355–364.
10. Derr LK (1998) The involvement of cellular recombination and repair genes in RNA-mediated recombination in *Saccharomyces cerevisiae*. *Genetics* 148(3):937–945.
11. Irimia M, Roy SW (2014) Origin of spliceosomal introns and alternative splicing. *Cold Spring Harb Perspect Biol* 6(6):a016071.
12. Sakurai A, et al. (2002) On biased distribution of introns in various eukaryotes. *Gene* 300(1-2):89–95.
13. Roy SW, Gilbert W (2005) The pattern of intron loss. *Proc Natl Acad Sci USA* 102(3):713–718.
14. Sverdlov AV, Babenko VN, Rogozin IB, Koonin EV (2004) Preferential loss and gain of introns in 3′ portions of genes suggests a reverse-transcription mechanism of intron insertion. *Gene* 338(1):85–91.
15. Roy SW, Irimia M (2009) Mystery of intron gain: New data and new models. *Trends Genet* 25(2):67–73.
16. Yenerall P, Zhou L (2012) Identifying the mechanisms of intron gain: Progress and trends. *Biol Direct* 7:29.
17. Tseng CK, Cheng SC (2008) Both catalytic steps of nuclear pre-mRNA splicing are reversible. *Science* 320(5884):1782–1784.
18. Rogozin IB, Carmel L, Csuros M, Koonin EV (2012) Origin and evolution of spliceosomal introns. *Biol Direct* 7:11.
19. Sorenson MR, Stevens SW (2014) Rapid identification of mRNA processing defects with a novel single-cell yeast reporter. *RNA* 20(5):732–745.
20. Curcio MJ, Garfinkel DJ (1991) Single-step selection for Ty1 element retrotransposition. *Proc Natl Acad Sci USA* 88(3):936–940.
21. Horecka J, Jigami Y (2000) Identifying tagged transposon insertion sites in yeast by direct genomic sequencing. *Yeast* 16(10):967–970.
22. Puig O, et al. (2001) The tandem affinity purification (TAP) method: A general procedure of protein complex purification. *Methods* 24(3):218–229.
23. Ghaemmaghami S, et al. (2003) Global analysis of protein expression in yeast. *Nature* 425(6959):737–741.
24. Klinz FJ, Gallwitz D (1985) Size and position of intervening sequences are critical for the splicing efficiency of pre-mRNA in the yeast *Saccharomyces cerevisiae*. *Nucleic Acids Res* 13(11):3791–3804.
25. Spingola M, Grate L, Haussler D, Ares M, Jr (1999) Genome-wide bioinformatic and molecular analysis of introns in *Saccharomyces cerevisiae*. *RNA* 5(2):221–234.
26. Bitter GA, Egan KM (1984) Expression of heterologous genes in *Saccharomyces cerevisiae* from vectors utilizing the glyceraldehyde-3-phosphate dehydrogenase gene promoter. *Gene* 32(3):263–274.
27. Truong LN, et al. (2013) Microhomology-mediated end joining and homologous recombination share the initial end resection step to repair DNA double-strand breaks in mammalian cells. *Proc Natl Acad Sci USA* 110(19):7720–7725.
28. Newman AJ, Norman C (1992) U5 snRNA interacts with exon sequences at 5′ and 3′ splice sites. *Cell* 68(4):743–754.
29. Newman AJ, Teigelkamp S, Beggs JD (1995) snRNA interactions at 5′ and 3′ splice sites monitored by photoactivated crosslinking in yeast spliceosomes. *RNA* 1(9):968–980.
30. van der Burgt A, Severing E, de Wit PJ, Collemare J (2012) Birth of new spliceosomal introns in fungi by multiplication of introner-like elements. *Curr Biol* 22(13):1260–1265.
31. Worden AZ, et al. (2009) Green evolution and dynamic adaptations revealed by genomes of the marine picoeukaryotes *Micromonas*. *Science* 324(5924):268–272.
32. Li W, Tucker AE, Sung W, Thomas WK, Lynch M (2009) Extensive, recent intron gains in *Daphnia* populations. *Science* 326(5957):1260–1262.
33. Simmons MP, et al. (2015) Intron invasions trace algal speciation and reveal nearly identical arctic and antarctic *Micromonas* populations. *Mol Biol Evol* 32(9):2219–2235.

GENETICS